SLAC-PUB-1689
December 1975
(T/E)

THE PHOTOPRODUCTION OF ψ, ψ' AND A SEARCH FOR NEW PARTICLES AT SLAC*

R. Prepost**

University of Wisconsin, Madison, Wisconsin, USA

The organization of this talk is as follows:

I. LIMITS ON RESONANT DILEPTON PRODUCTION OTHER THAN ψ

SLAC-UMASS-MIT Experiment
DESY Experiment

II. THE SLAC-WISCONSIN EXPERIMENT $\gamma N \rightarrow \psi, \psi'$

Double Arm ψ Production
Single Arm ψ Production

III. THE INELASTIC CROSS SECTION AND LIMITS ON D PRODUCTION

I. LIMITS ON RESONANT DILEPTON PRODUCTION OTHER THAN ψ

Two contributions have been submitted to this conference which set limits for dilepton narrow mass peaks in the mass range from 1 - 2.7 GeV. The first experiment was carried out by a SLAC-UMASS-MIT Collaboration (paper 145) at SLAC and is an experiment designed to detect muon pairs in the 1 - 3 GeV mass range from 20 GeV electrons incident on a Be target. No narrow peaks were observed in the mass interval from 1 to 2.7 GeV and the authors quote the following 90% confidence limits:

$$\sigma\ BR < .05 \times 10^{-33} cm^2 \quad \text{at } M = 2.7 \text{ GeV}$$
$$\sigma\ BR < .16 \times 10^{-33} cm^2 \quad \text{at } M = 1 \text{ GeV}$$

with the limits varying smoothly from M = 1 GeV to M = 2.7 GeV.

The second search for narrow dilepton states was carried out by a DESY Group (paper 185) detecting e^+e^- from a 7 GeV end point bremsstrahlung beam incident on a Be target. No narrow peaks were observed, and the authors quote a 90% confidence limit for the mass range 2.1 GeV $\leq$ M $\leq$ 2.6 GeV of σ BR < $0.2 \times 10^{-34} cm^2$.

Therefore, there is no evidence for narrow dilepton resonances other than the $\psi(3.1)$ in the mass range from ~ 1 - 3 GeV.

---

*Work supported by the U.S. Energy Research and Development Administration.
**This paper was written while the author was in residence at the Stanford Linear Accelerator Center, Stanford, California.

(Presented at the International Symposium on Lepton and Photon Interactions, Stanford University, Stanford, California, August 21-27, 1975)

II. THE SLAC-WISCONSIN EXPERIMENT FOR ψ, ψ' PHOTOPRODUCTION[1]

I will now turn to a discussion of the photoproduction experiment carried out at SLAC for $\psi(3.1)$ and $\psi(3.7)$ production. The experiment was carried out by a SLAC-Wisconsin collaboration.

SLAC	Wisconsin
R. L. Anderson	U. Camerini
W. W. Ash	J. G. Learned
D. M. Ritson	R. Prepost
D. J. Sherden	C. M. Spencer
C. K. Sinclair	D. E. Wiser

The Double Arm ψ, ψ' Measurements

Most of the measurements carried out in this experiment were of $\psi(3.1)$ and $\psi(3.7)$ production from a deuterium target using the SLAC 8 GeV and 20 GeV spectrometers in coincidence to detect both electron and muon pairs. The spectrometers themselves are focussing devices which give a momentum and production angle display of the detected particles. Most of the measurements were taken using a bremsstrahlung beam of $\sim 2 \times 10^{10}$ EQ/pulse intensity with ~ 120 pulses/sec but some measurements of $\psi(3.1)$ production were made using an electron beam. Almost all the measurements were made using a deuterium target in order to maximize the target thickness per radiation length, but one of the data points was also run using a hydrogen target.

The spectrometers were instrumented to detect both electrons and muons. A plan view of the experimental set up is shown in Fig. 1. The electron

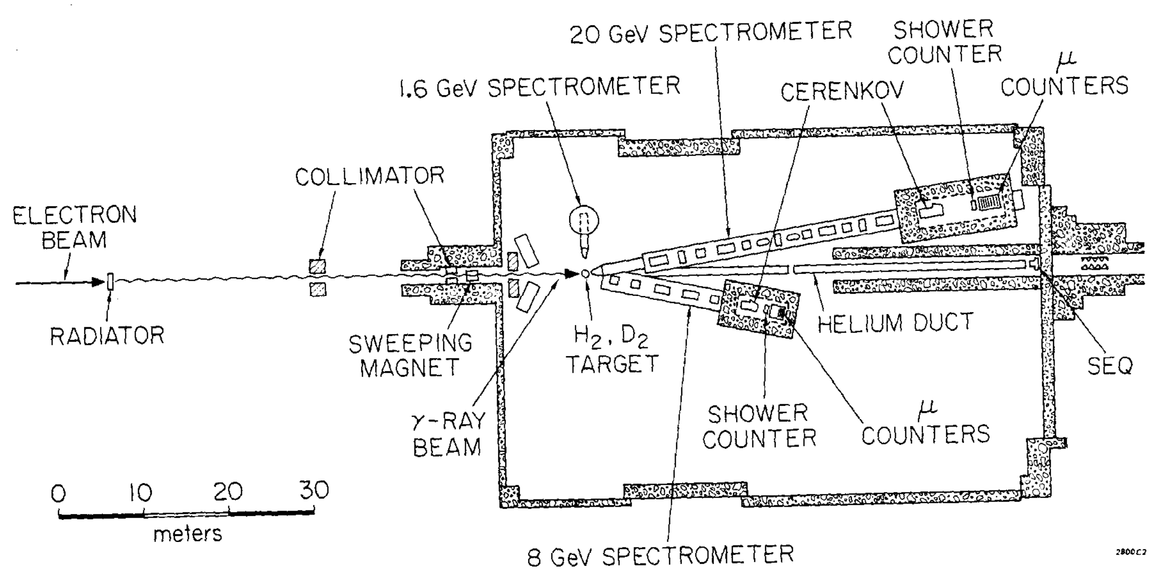

Fig. 1. Plan view of experimental set up for studying the reaction $\gamma N \to \psi X$.

identification was made by a combination of a threshold Cerenkov counter, a lead glass preradiator, and a lead lucite shower counter. Muons were identified by a scintillation counter array behind approximately 1.3 m of iron. In addition, each spectrometer was instrumented with momentum and production angle hodoscopes capable of measuring momenta to $(\Delta p/p) = \pm 0.1\%$ and production angles to $\Delta\theta \simeq \pm 0.15$ mr. The hodoscopes were used to sample the invariant mass distribution of the detected pairs within the spectrometer acceptance.

Some details of the apparatus are as follows: The mass acceptance of the apparatus was $\Delta M/M \simeq .05$ (FWHM) with the hodoscopes giving a mass resolution within the full acceptance of $\delta M \simeq 20$ MeV (FWHM) at $M = 3.1$ GeV. The ψ energy acceptance was $\Delta E_\psi/E_\psi \simeq .02$ (FWHM) which is also approximately $\Delta k/k$ for elastic production where k is the photon energy. The momentum transfer acceptance was $\Delta p_\perp^2 \simeq .03\ (\mathrm{GeV/c})^2$ at $E_\psi = 20$ GeV and $\theta_\psi = 0$. The apparatus was set to detect lepton pairs near 90° in the rest frame of the ψ particle and the apparatus detected a fraction of the ψ decay cone given by

$$\int dn/d\Omega^* \, d\Omega^* \simeq 4 \times 10^{-4}.$$

Data were taken for a variety of spectrometer settings. Each spectrometer setting corresponded to a relatively small acceptance in photon energy and momentum transfer. The data points included $\psi(3.1)$ production for photon energies k = 13, 15, 16, 17, 19 and 21 GeV and $\psi'(3.7)$ production at k = 21 GeV at the minimum momentum transfer, (i.e., $\theta_\psi = 0$). At 19 GeV three points on an angular distribution were taken for $(t - t_{min}) = 0$, 0.2, and 0.4 $(\mathrm{GeV/c})^2$.

Some inelasticity studies were made at k = 19 GeV and k = 15 GeV. All of the above data points were taken using a deuterium target, and a hydrogen-deuterium comparison was made at 19 GeV. In each case the spectrometers were set to detect psi decays near 90° in the psi rest frame with respect to the beam direction.

The kinematic acceptance of the apparatus with respect to the photon energy producing the detected psi particles is a somewhat confusing point and requires some clarification. This will be done with reference to Fig. 2 which shows the acceptance for various data point conditions on a Peyrou plot. The spectrometers are set to detect a given psi energy and angle within ΔE_ψ and $\Delta\theta_\psi$. The bremsstrahlung end point energy E_0 is an additional experimental variable and determines the range of photon energies and hence range of recoil

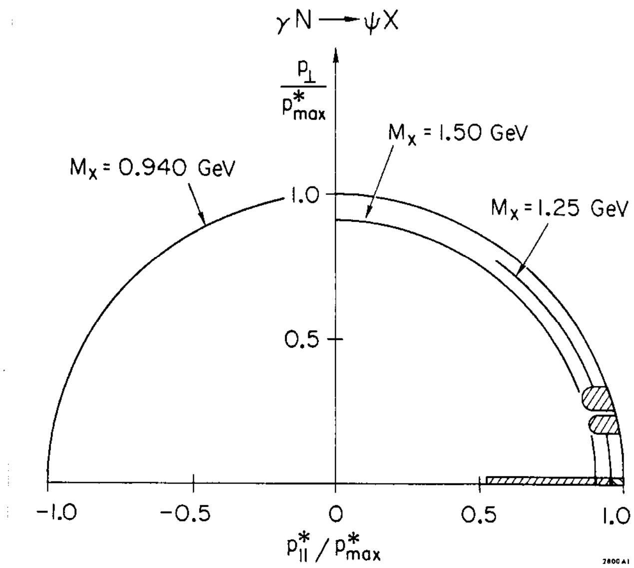

Fig. 2. Peyrou plot for the reaction $\gamma N \to \psi X$ showing data point conditions.

masses that can contribute to the reaction $\gamma N \to \psi X$. The range of photon energies and recoil masses than can contribute to a given data point ranges from $k = E_\psi$, $M_X = M_N$ to $k = E_0$ and whatever recoil mass M_X this corresponds to. As $(E_0 - E_\psi)$ approaches zero, the production is kinematically constrained to be elastic production. Figure 2 shows where the data points of this experiment lie on a normalized Peyrou plot. Each data point corresponds to a shaded region on the plot. The plot also shows the extreme recoil mass contour for $(E_0 - E_\psi) = 1.0$ GeV at $M_X = 1.5$ GeV. Thus the recoil mass acceptance ranges from $M_X = M_N = .94$ GeV to $M_X = 1.5$ GeV when $(E_0 - E_\psi) = 1.0$ GeV and is correspondingly smaller for $(E_0 - E_\psi) = 0.5$ GeV. The only other data point condition which was run besides $(E_0 - E_\psi) = 0.5$ and 1.0 GeV was $(E_0 - E_\psi) = 5$ GeV at $E_\psi = 15$ GeV, and the acceptance for this data point is shown by the long shaded area on the $p_\perp = 0$ axis. In this case the recoil mass acceptance ranges from $M_X = 0.94$ GeV to $M_X \simeq 2.6$ GeV. The points which were run for other than t_{min} momentum transfer were for $(E_0 - E_\psi) = 1.0$ GeV, and their acceptance is shown by the shaded regions off the $p_\perp = 0$ axis. Thus the data points are constrained to lie within a narrow region about the elastic production boundary when $(E_0 - E_\psi) = 0.5$ and 1.0 GeV, and a direct determination of inelastic contributions can be made by fixing E_ψ and varying E_0. If this change does not result in a change in yield, than the production is predominantly elastic production. For this experiment, the largest change was made by fixing $E_\psi = 15$ GeV and measuring yields for both $E_0 = 16$ GeV and $E_0 = 20$ GeV.

Some other kinematic features of these measurements are also quite relevant for the determination of cross sections. One is the fact that the large t_{min} of the psi production ensures that the production from deuterium will be primarily incoherent production. Secondly, the kinematic conditions for the

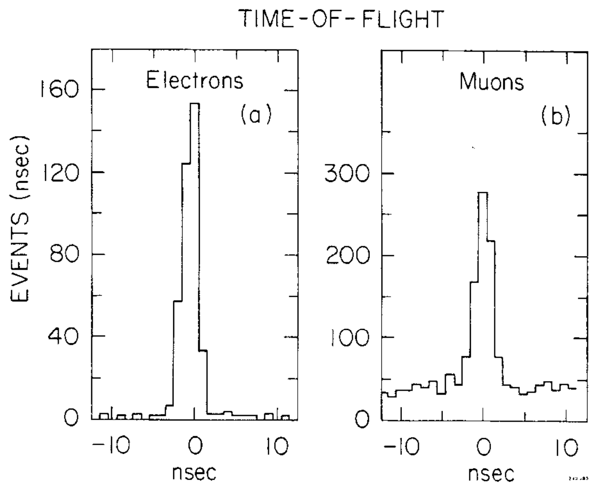

Fig. 3. Time-of-flight distributions between the spectrometers for electrons (a) and muons (b).

case of operating 0.5 GeV or 1.0 GeV from the bremsstrahlung end point are such that $\psi(3.1)$ production from the cascade decay of the $\psi(3.7)$ is heavily suppressed.

I will next discuss the quality of the observed psi signal. Figures 3a and 3b show time-of-flight distributions between the two spectrometers for both electron and muon triggers for a large sample of the $\psi(3.1)$ data. The random background is typically 1% for electron pairs and 20 - 30% for muon pairs. The random background is higher for muons than for electrons since most of the muons detected by the apparatus are from pion decay. Figures 4a and 4b show the ee and $\mu\mu$ invariant mass distributions for a sample of $\psi(3.1)$ events which gave good hodoscope patterns. Events which did not give good hodoscope patterns were generally associated with one or more extra random tracks in the hodoscopes, or were events which gave no hodoscope pattern at all since the trigger counter acceptance was larger than that of the hodoscopes.

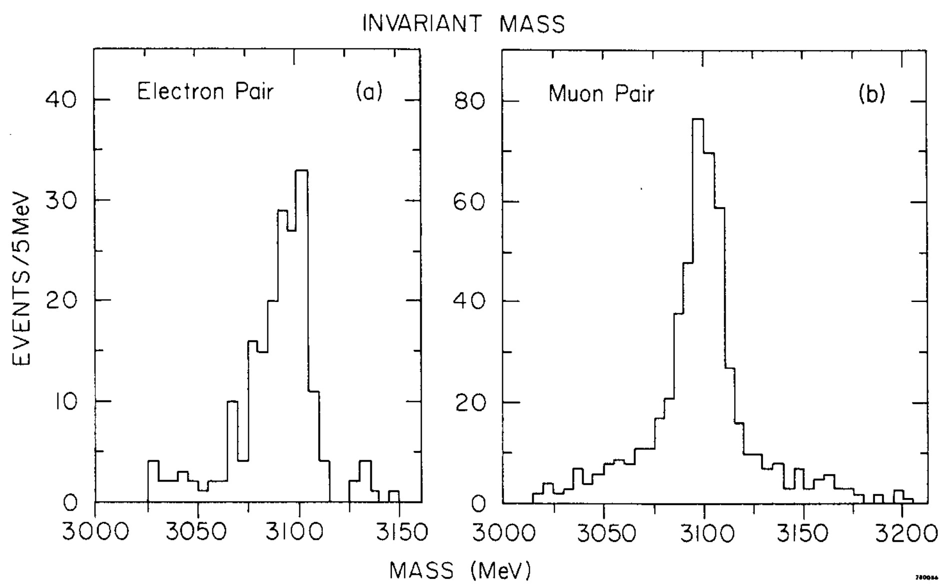

Fig. 4. Invariant mass distributions for a sample of $\psi(3.1)$ events for electrons (a) and muons (b).

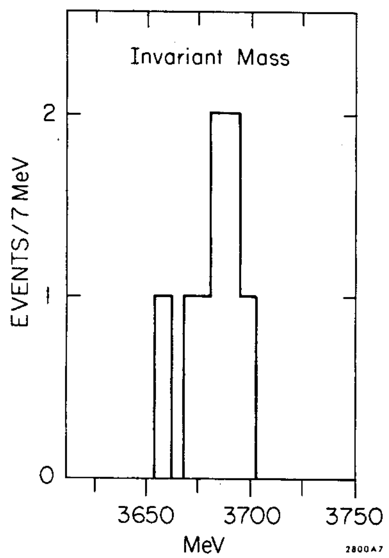

Fig. 5. Invariant mass distribution for a sample of $\psi(3.7)$ events containing both electron and muon events.

Figure 5 shows the combined muon and electron pair data for $\psi(3.7)$ events which gave a reconstructable mass. The mass plot contains 8 events and a negligible random background.

Cross sections were determined by using the full aperture trigger counter event rate together with the time-of-flight distributions for random background subtraction. The following assumptions were made for cross section determinations:

a. The yields are due to elastic psi production, i.e., $\gamma N \to \psi N$.

b. The branching ratios for decay into e or μ pairs are 6.9% and 1% for the $\psi(3.1)$ and $\psi(3.7)$, respectively.

c. The psi particles decay with a $(1 + \cos^2\theta^*)$ distribution in their own rest frame. (The data points correspond to $\theta^* \simeq 90^\circ$.)

The cross section results are based on approximately 1200 $\psi(3.1)$ events and 13 $\psi(3.7)$ events. At high energies where kinematic factors are favorable, yields of 70 - 90 $\psi(3.1)$ events per day were obtained. The measured muon pair yields was approximately a factor 1.7 greater than the electron pair yield. When the data are corrected for the trigger counter acceptances and for radiative corrections, the muon and electron yields are equal within the estimated systematic and statistical errors. Yields from the $\psi(3.7)$ were much smaller, primarily due to the smaller branching ratio into lepton pairs.

The results are presented in Table I and Fig. 6 and 7. Table I lists the conditions for which data were taken and the corresponding values of $d\sigma/dt$. The errors indicated in Table I are statistical only. The systematic error for the electron yields is dominated by the correction for radiative losses, and for the muons is primarily from the uncertainty in solid angle. The overall systematic error for the cross sections is estimated to be 15%. In order to compare cross sections as a function of energy, the t_{min} data have been extrapolated to $t = 0$ by the correction factor $\exp(-bt_{min})$ with $b = 2.9\ (\mathrm{GeV}/c)^{-2}$.

Table I

k (GeV)	E_0 (GeV)	t_{min} $(GeV/c)^2$	t' $(GeV/c)^2$	$d\sigma/dt(t)$ $[nb/(GeV/c)^2]$
a. ψ(3100) from Deuterium Target				
21.0	21.5	0.069	0.0	14.6 ± 1.2
19.0	20.0	0.088	0.0	15.0 ± 1.0
19.0	19.5	0.088	0.0	12.0 ± 1.1
17.0	17.5	0.116	0.0	10.8 ± 1.0
16.0	16.5	0.135	0.0	8.2 ± 1.1
15.0	20.0	0.160	0.0	7.7 ± 1.5
15.0	16.0	0.160	0.0	5.9 ± 1.0
13.0	13.5	0.236	0.0	3.8 ± 0.8
19.0	20.0	0.088	0.20	8.2 ± 1.1
19.0	20.0	0.088	0.40	4.9 ± 0.7
b. ψ(3100) from Hydrogen Target				
19.0	19.5	0.088	0.0	10.8 ± 1.1
c. ψ(3700) from Deuterium Target				
21.0	21.5	0.164	0.0	2.1 ± 0.8

$t' \equiv (t - t_{min})$

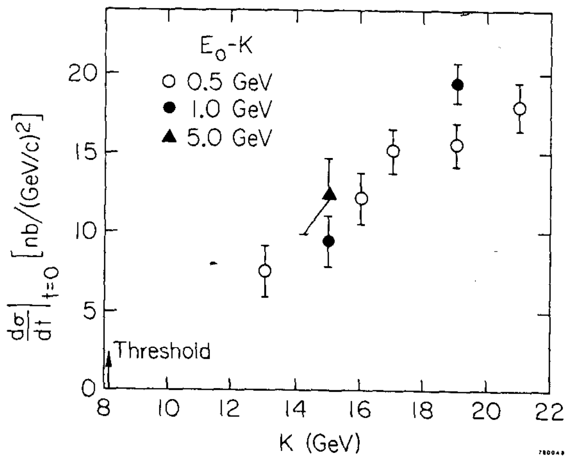

Fig. 6. Cross section for $\gamma N \rightarrow \psi N$ extrapolated to t = 0 for $\psi(3.1)$ production as a function of photon energy.

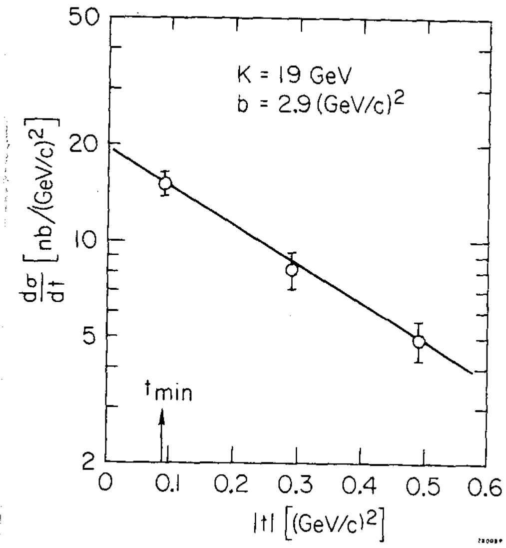

Fig. 7. Differential cross section for $\psi(3.1)$ production for k = 19 GeV and E_0 = 20 GeV as a function of t.

The resultant $\psi(3.1)$ t = 0 cross sections are shown as a function of photon energy in Fig. 6. Figure 7 shows the k = 19 GeV, E_0 = 20 GeV data points as a function of t.

Let me now discuss the main features of the results.

1. The masses determined from the hodoscope mass distributions are

$$M(3.1) = 3098 \pm 6 \text{ MeV}$$
$$M(3.7) = 3684 \pm 9 \text{ MeV}.$$

2. A comparison of data taken with different bremsstrahlung end point energies indicates a possible 20 - 30% inelastic contribution at t_{min} (see Table I).
3. Psi production from the neutron and proton are very similar. The $\psi(3.1)$ production per nucleon from hydrogen and deuterium is

$$\sigma(D)/\sigma(H) = 1.12 \pm .16 \quad \text{at } k = 19 \text{ GeV}, \; t_{min}.$$

4. The $\psi(3.7)$ is photoproduced. Assuming a 1% branching ratio into e or μ pairs, the cross section ratio at $k = 21$ GeV, t_{min} is

$$\frac{\sigma(3.1)}{\sigma(3.7)} = 6.8 \pm 2.4.$$

One should keep in mind that t_{min} is quite different for $\psi(3.1)$ and $\psi(3.7)$.

5. The slope of the angular distribution measured at $k = 19$ GeV has a fitted slope parameter $b = 2.9\ (\text{GeV/c})^{-2}$ where b is defined by $d\sigma/dt \sim \exp(bt)$. The statistical error from the fit is $\pm\ 0.3\ (\text{GeV/c})^{-2}$ but here one should keep in mind that the inelasticity of the production has not been determined at other than t_{min} and the true elastic slope may be larger than the above quoted value.
6. If the photoproduction of the psi is assumed to be psi dominated (in analogy to the usual vector dominance arguments), then

$$d\sigma/dt(\gamma N \to \psi N) = \left(3\Gamma_{\psi \to ee}/\alpha M_{\psi}\right) d\sigma/dt(\psi N \to \psi N)$$

where $\Gamma_{\psi \to ee}$ is the partial rate of $\psi \to ee$ as determined by the storage ring results. Further use of the optical theorem then yields:

$$d\sigma/dt\,\Big|_{t=0}(\gamma N \to \psi N) = \left(3\Gamma_{\psi \to ee}/16\pi\alpha M_{\psi}\right) \sigma^2_{TOT}(\psi N)(1 + \beta^2)$$

where $\beta = \frac{\text{ReA}}{\text{ImA}}$ and A is the forward elastic scattering amplitude. A plot of $\sigma_{TOT}(\psi N)$ ($\beta = 0$ is assumed) versus s is shown in Fig. 8 for the data of this experiment as well as the FNAL and Cornell points which have been reported at this conference. (See the reports of W. Lee[2] and B. Gittelman presented at this conference.) The figure also shows

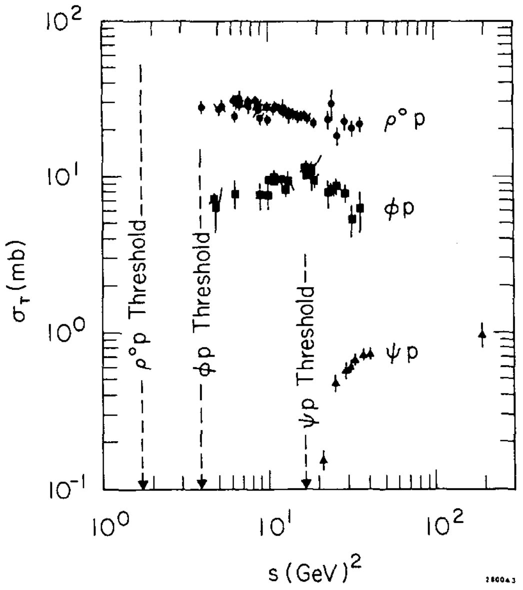

Fig. 8. $\sigma_{TOT}(\psi N)$, $\sigma_{TOT}(\phi N)$, and $\sigma_{TOT}(\rho N)$ cross sections for all available experimental data as a function of s. The FNAL and Cornell points for $\psi(3.1)$ production have been included on the plot.

the corresponding data extracted from $\gamma N \to \rho N$ and $\gamma N \to \phi N$ experiments. It is apparent that $\sigma_{TOT}(\psi N)$ is appreciably smaller than either $\sigma_{TOT}(\rho N)$ or $\sigma_{TOT}(\phi N)$ with an asymptotic value of ~ 1 mb. However, it should be emphasized that the extraction of $\sigma_{TOT}(\psi N)$ in this fashion depends upon the assumptions mentioned above. The use of $\Gamma_{\psi \to ee}$ from storage ring data presumes an extrapolation from $Q^2 = M_\psi^2$ to $Q^2 = 0$, and the use of the optical theorem assumes $\beta = 0$. It should, however, be possible to obtain independent $\sigma_{TOT}(\psi N)$ information from a measurement of the A dependence of the $\gamma N \to \psi N$ cross section.

Single Arm Psi Production

During the course of this experiment some measurements were made of direct electron production in the reaction $\gamma N \to e^{\pm} X$. These measurements were made using the 20 GeV spectrometer and consisted of measuring the electron yield for a fixed spectrometer momentum of p = 6.0 GeV/c with a 21.5 GeV bremsstrahlung beam and varying spectrometer angles covering the $p_\perp$ range from 0.6 - 1.8 GeV/c. In addition, for each point, radiator extrapolations were made in order to isolate the direct electron component. What one expects to see in a scan like this is an electron yield consisting of direct electrons, and electrons produced by gamma ray conversion in the target. The electrons produced by gamma conversion arise primarily from $\pi^0 \to \gamma\gamma$ decays with conversion of one of the gamma rays in the target. This component can be experimentally isolated by extrapolating to zero radiator thickness. The direct electron signal includes Bethe-Heitler pair production, $\pi^0 \to \gamma ee$ Dalitz decays, and other sources of direct electrons from particle decays such as vector meson decays into electron-positron pairs. At large values of transverse momentum ($p_\perp > 1.5$ GeV/c), one would expect this component to be dominated by psi production since the psi's are the only known resonances

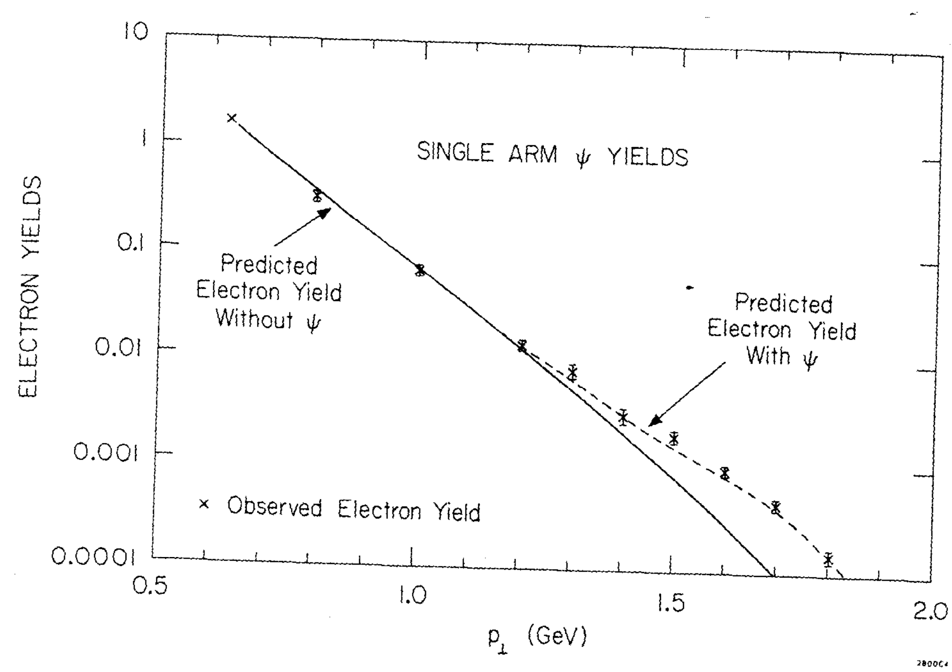

Fig. 9. Single arm electron yields as a function of transverse momentum for p_{spect} = 6.0 GeV and E_0 = 21.5 GeV.

with a large enough mass to produce abundant large $p_\perp$ electrons or positrons. The direct electron component from psi decay should manifest itself by a shoulder or step in the transverse momentum distribution of the electron yield when $p_\perp \simeq M_\psi/2 = 1.5$ GeV/c is reached. Figure 9 shows the results of such a transverse momentum yield curve. Each data point consisted of a set of measurements with varying converter thickness for the radiator extrapolation. The yield curve shows the observed total electron yield data points, and the dashed and solid lines show the predicted electron yield with and without a $\psi(3.1)$ contribution respectively. The predicted electron yields below $p_\perp \simeq 1.2$ GeV/c were based on calculated Bethe-Heitler yields and a π^0 contribution based on the measured converted photon yields. At $p_\perp \geq 1.4$ GeV/c the $\psi(3.1)$ contribution becomes evident, and at $p_\perp = 1.5$ GeV/c actually dominates the measured electron yield with ~ 60% of the measured yield coming from $\psi \to e^+e^-$ decays. The dashed line is the predicted electron yield based on all sources including a $\psi(3.1)$ contribution based on the results of the double arm measurements. The charged pion yields were also simultaneously measured, and for $p_\perp = 1.5$ GeV/c we find that

$$\frac{\psi \to e^-}{\pi^-} \simeq \frac{1}{750}$$

and

$$\frac{\psi \to e}{\text{All } e} \simeq 0.60.$$

That is to say, electrons from psi decay dominates the electron yield at large transverse momentum and are approximately 10^{-3} of the charged pion yield at the same $p_\perp$.

III. THE INELASTIC CROSS SECTION AND LIMITS ON D PRODUCTION

This section contains some remarks about the inelastic cross section which may be associated with elastic psi production, and some experimental limits on D photoproduction obtained during this experiment by looking for double arm hadron coincidences in the M = 2.0 GeV region and direct single arm electrons in the $p_\perp$ = 1.0 GeV/c region.

The inelastic cross section associated with $\gamma N \to \psi N$ production may be simply estimated as follows: If the optical theorem is assumed to apply to $\gamma N \to \psi N$ and the corresponding inelastic processes, then from the optical theorem $\sigma_{el} = \frac{1}{16\pi b}\ \sigma^2_{TOT}$ we can write

$$\frac{\sigma_{el}}{\sigma_{TOT}} = \frac{1}{16\pi b}\ \sigma_{TOT}.$$

If for the right hand side we set $\sigma_{TOT}(\psi N) \simeq 1$ mb and use the elastic slope $b = 3(\text{GeV/c})^{-2}$, then we can evaluate σ_{el}/σ_{TOT}, and by vector dominance the ratio should be the same for both psi initiated and photon initiated reactions. This yields $\sigma_{el}/\sigma_{TOT} \simeq 10^{-2}$ and since

$$\sigma_{TOT} = \sigma_{el} + \sigma_{in}\ ,\ \frac{\sigma_{el}}{\sigma_{TOT}} \simeq \frac{\sigma_{el}}{\sigma_{in}} \simeq 10^{-2}.$$

From the experiment described in this report we know that inelastic psi production is small, certainly not larger than elastic psi production, and most probably ≤ 20 - 30% of the elastic production. Therefore the large predicted inelastic cross section of $\sigma_{in} \simeq 0.5$ μb based on $\sigma_{el} \simeq 5$ nb does not involve $\psi(3.1)$'s in the final state. This large inelastic cross section is ~ 1/2% of the total $\sigma_{\gamma N}$ cross section and is an enormous cross section. What are the candidates? The most likely possibility in the spirit of charmed quarks is $\gamma N \rightarrow D\bar{D}N$ where D here is simply a generic symbol for charmed mesons. In this regard one should look back at Fig. 8, the plot of $\sigma_{TOT}(\psi N)$ versus s. Since the elastic production is presumed to be the shadow of inelastic processes there may be a threshold effect for σ_{el} when the real inelastic channels open up. Figure 8 indicates that the effective σ_{el} threshold is above the real physical threshold for $\gamma N \rightarrow \psi N$. This statement depends very crucially upon precise $\gamma N \rightarrow \psi N$ measurements near threshold, and will be a subject for further experiments. However, the evidence is tantalizing that an inelastic threshold is opening up at $\sqrt{s} \simeq 4.6$ GeV corresponding to a D mass of ~ 1.8 GeV.

Finally, I will describe the experimental limits on charmed meson production obtained during the course of this experiment. Two such searches were made, one looking for hadron double arm coincidences in the M = 1.8 - 2.4 GeV region, and the other a search for excess direct electrons in the $p_\perp = 0.6$ - 1.0 GeV/c region.

The double arm hadron measurements were sensitive to πK, $\pi\pi$, KK, πp, and $p\bar{p}$ coincidences, but particles were only identified as π or non π. The mass range 1.8 GeV $\leq M_{hh} \leq$ 2.4 GeV was covered in overlapping steps. Typical experimental parameters were $\theta_8 = \theta_{20} \simeq 12^\circ$ and $p_8 = p_{20} \simeq 4.7$ GeV/c. Because of the increased random background resulting from the high rate hadron fluxes, this scan was run with 100X less cross section sensitivity than the ee and μμ psi cross section measurements. No real events were observed and the approximate cross section limit is

$$\mathrm{BR}\ d\sigma/dp_\perp^2 dx \leq 0.5\ \mu b/(\mathrm{GeV}/c)^2.$$

If an $\exp(-5p_\perp^2)$ dependence is assumed, then

$$\mathrm{BR}\sigma \leq 0.1\ \mu b = 10^{-31} \mathrm{cm}^2$$

or

$$\frac{\mathrm{BR}\sigma}{\sigma_{TOT}(\gamma N)} \leq 10^{-3}$$

where BR is the branching ratio of D into the detected hadron channel.

The direct excess electron search is based on the data of Fig. 9 which were examined for excess electrons in the $p_\perp = 0.6 - 1.0$ GeV/c region. The major background is from $\pi^0 \to \gamma\gamma \to ee\gamma$ conversions, but this contribution can be measured directly and inferred from the measured $\pi^\pm$ yields. There is no evidence for any excess direct electron signal beyond the mundane sources with a sensitivity set by the subtraction procedures. If the direct electrons are assumed to come via $\gamma N \to D\bar{D}N$ with $D \to Ke\nu$, then the limit obtained is $BR\sigma \leq 10^{-32} cm^2$. These limits will be substantially improved in subsequent running of this experiment.

Finally, I would like to acknowledge the considerable effort of my colleagues on the work of this experiment.

REFERENCES

1. U. Camerini et al., Phys. Rev. Letters 35, 483 (1975).
2. B. Knapp et al., Phys. Rev. Letters 34, 1040 (1975).

DISCUSSION

Note: The papers of W. Y. Lee, R. Prepost and B. Gittelman were discussed together at the conclusion of Gittelman's talk. See the report of this discussion at the end of Gittelman's paper.